Bioorganic Chemistry 87 (2019) 803–809

Contents lists available at ScienceDirect

Bioorganic Chemistry

journal homepage: www.elsevier.com/locate/bioorg

Mechanistic investigation of anthocyanidin derivatives as α-glucosidase inhibitors

Jang Hoon Kim, Hyo Young Kim, Chang Hyun Jin*

Advanced Radiation Technology Institute, Korea Atomic Energy Research Institute, Jeongeup 56212, Republic of Korea

ARTICLE INFO

Keywords:
Anthocyanidin derivative
α-Glucosidase
Mixed noncompetitive mode
In silico

ABSTRACT

Eight anthocyanidin derivatives (**1–8**) were evaluated as potential inhibitors of the catalysis of α-glucosidase. Among them, compounds **4** and **8** had the highest levels of inhibitory activity at 100 μM (IC_{50} values of 14.4 ± 0.1 and 29.7 ± 1.2 μM) and acted in a dose-dependent manner. Enzyme kinetic analysis further revealed that these inhibitors interacted with α-glucosidase in a mixed noncompetitive mode. Moreover, fluorescence quenching studies provided parameters for calculating the binding mechanism between receptor and ligand. On the basis of these studies, and *in silico* simulations, we determined that the ligand was likely docked in the receptor. Thus, compounds **4** and **8** are excellent potential targets for *in vitro* cell-based and *in vivo* assays related to treatment of diabetes.

1. Introduction

Anthocyanidins and anthocyanins (glycosides of anthocyanidins) are flavonoid phenolic compounds that are among the most common types of plant pigments [1]. They typically are responsible for the red, orange, blue, and violet colors in flowers, fruits, and vegetative tissues [1,2]. They are water soluble, with various biological activities, including antioxidant, anti-inflammatory, anti-cancer, and anti-diabetic activities [3], and they have been used as colorants in food and cosmetic products [4]. Among the various anthocyanins, cyanidin-3-*O*-glucoside has been shown to suppress reproductive toxicity induced by acrylamide and glycidamide in leydig cell [5]. Cyanidin was reported to down-regulate superoxide anion and hydroxyl radical generation in a lysine/methylglycoxal system [6]. Furthermore, anthocyanin derivatives are characterized by their different forms depending on the pH value of the solution. With a pH > 7, cyanidins are degraded to aldehydes and phenolic acids or changed with diketone [7].

α-Glucosidase (EC 3.2.1.20), which is located on the epithelium of the small intestine, is a hydrolase that converts starch and carbohydrates to glucose by reacting with 1,4-α linkages during digestion [8,9]. Free monosaccharides absorbed in the bloodstream can result in hyperglycemia caused by type-2 diabetes [9]. Therefore, the development of α-glucosidase inhibitors, such as acarbose, voglibose, and miglitol, has been critical treatments for type-2 diabetes by reducing postprandial hyperglycemia [8,9]. In 2014, there were 422 million diabetics, and in 2015, there were 1.6 million reported deaths directly from this disease [10]. In a 2012 report, type-2 diabetes is found in 90% of all diabetics [11]. By 2030, the World Health Organization predicts that diabetes will be the seventh leading cause of death [10]. Therefore, additional treatments will be necessary to combat the growing incidence of this disease. Recently, anti-diabetic inhibitors have been developed flavonoids from natural plants [12]. Kaempferol, quercetin, luteolin, quercetin 3-*O*-(6-*O*″-galloyl)-β-glucopyranoside and 3,7,8,3′,4′-pentahydroxyflavone has showed potential inhibitory activities to prevent the catalytic reaction of α-glucosidase [12,13]. These inhibitors are similar to the anthocyanin structure except for the difference in the positive charge of oxygen of the C-ring of flavonoids [14].

In this study, we investigate the potential α-glucosidase inhibitory activity of anthocyanin derivatives. Using enzyme kinetics, fluorescence quenching, and molecular docking studies, we have identified two compounds anthocyanin compounds that show a dramatic decrease in turnover rate of the catalytic reaction. In addition, we reveal the binding mechanisms for how they bind to α-glucosidase, providing a potentially powerful additional natural compound for developing treatment for type-2 diabetes.

2. Results and discussion

2.1. α-Glucosidase inhibitory assay

Anthocyanin-rich fractions are known to have a high inhibitory activity on α-glucosidase [15]. However, cyanidin, cyanidin-3-*O*- β-

* Corresponding author.
E-mail address: chjin@Kaeri.re.kr (C.H. Jin).

https://doi.org/10.1016/j.bioorg.2019.01.033
Received 19 November 2018; Received in revised form 7 January 2019; Accepted 21 January 2019
Available online 22 January 2019

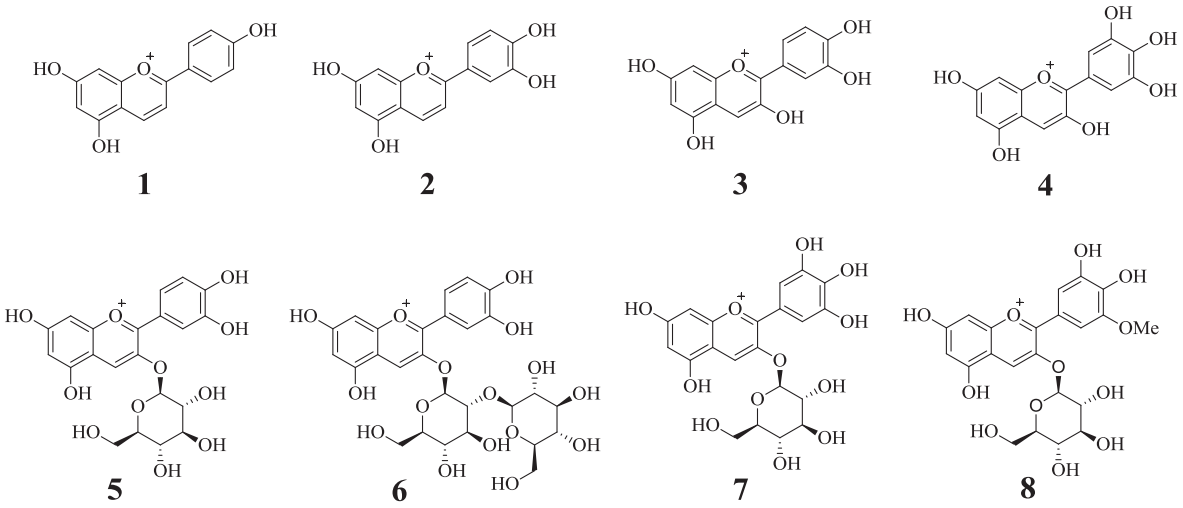

Fig. 1. Structures of anthocyanidin derivative (**1–8**).

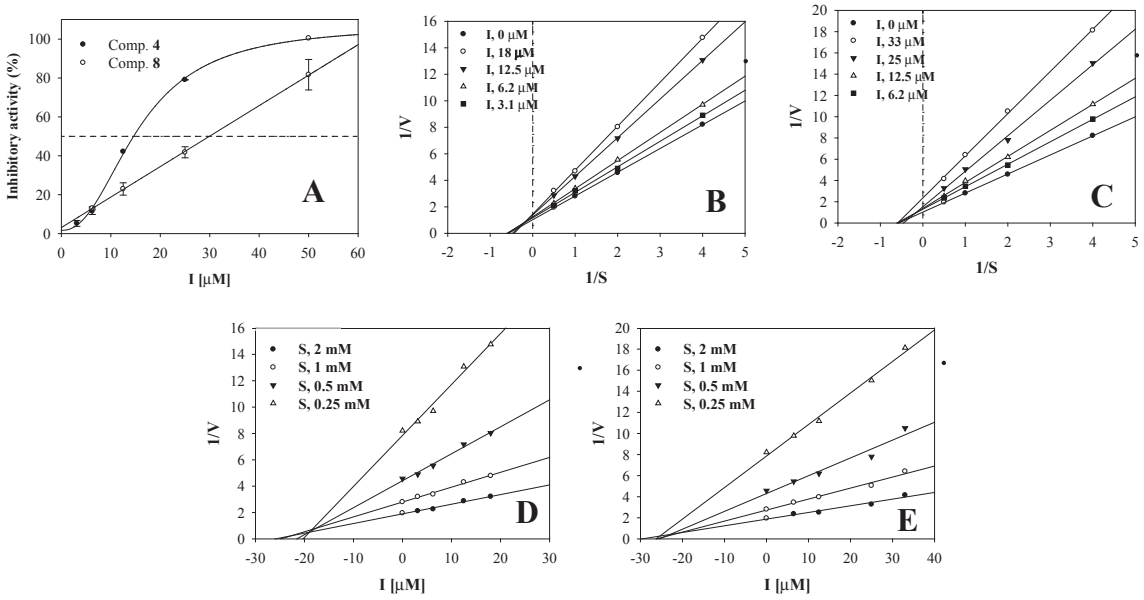

Fig. 2. Inhibitory activity ranging from 6.2 to 50 μM (A) of α-glucosidase. Lineweaver–Burk plots (B and C) and Dixon plots (D and E) were constructed from the inhibition of α-glucosidase by compounds **4** and **8**.

Table 1
α-Glucosidase inhibitory effect of anthocyanin derivative (**1–8**).

Inhibition of compounds on α-glucosidase[a]		
Compounds	IC_{50} (μM)	Binding Mode (k_i, μM)
1	N.T[c]	N.T[c]
2	N.T[c]	N.T[c]
3	N.T[c]	N.T[c]
4	14.4 ± 0.1	Mixed (18.5 ± 1.4)
5	N.T[c]	N.T[c]
6	N.T[c]	N.T[c]
7	N.T[c]	N.T[c]
8	29.7 ± 1.2	Mixed (24.3 ± 2.1)
Acarbose[b]	210.8 ± 4.6	

[a] Compounds were tested three times.
[b] Positive control.

glucoside, cyanidin-3,5-*O*- β-diglucoside, and cyanidin-3-*O*- β-rutinoside have been reported recently to have low IC_{50} values at concentrations greater than 100 μM [16]. These facts led us to investigate enzyme inhibitory activities of other anthyocyanin derivatives, identified as apigeninidin (**1**), luteolinidin (**2**), cyanidin (**3**), delphinidin (**4**), kuromanin (**5**), cyanidin-3-*O*-β-sophoroside (**6**), delphinidin-3-*O*-β-glucoside (**7**), and peturidin-3-*O*-glucoside (**8**) (Fig. 1). Among them, two compounds (**4** and **8**) had inhibitory effects of over 50% within 100 μM concentration. These compounds suppress the catalytic reaction at concentrations ranging from 3.1 to 50 μM, in a dose-dependent manner, with the IC_{50} values of 14.4 ± 0.1 and 29.7 ± 1.2 μM, respectively (Fig. 2A and Table 1). The positive control used was acarbose with an IC_{50} value of 210.8 ± 4.6 μM (Table 1).

Furthermore, to identify the binding mechanism of α-glucosidase to the ligands (compounds **4** and **8**), we tested the initial velocity (v_0) of substrate conversion by the enzyme at different concentrations of inhibitor depending on various substrate concentrations. Calculated v_0 values versus substrate concentration were converted to a Linewear–Burk plot. Two compounds (**4** and **8**) were nearly linear but with different slopes and intercepts. This study showed that the inhibitors repressed α-glucosidase activity with the mixed non-competitive type (Fig. 2B and C and Table 1). Furthermore, Dixon plots indicated that compounds **4** and **8** had k_i respective values of

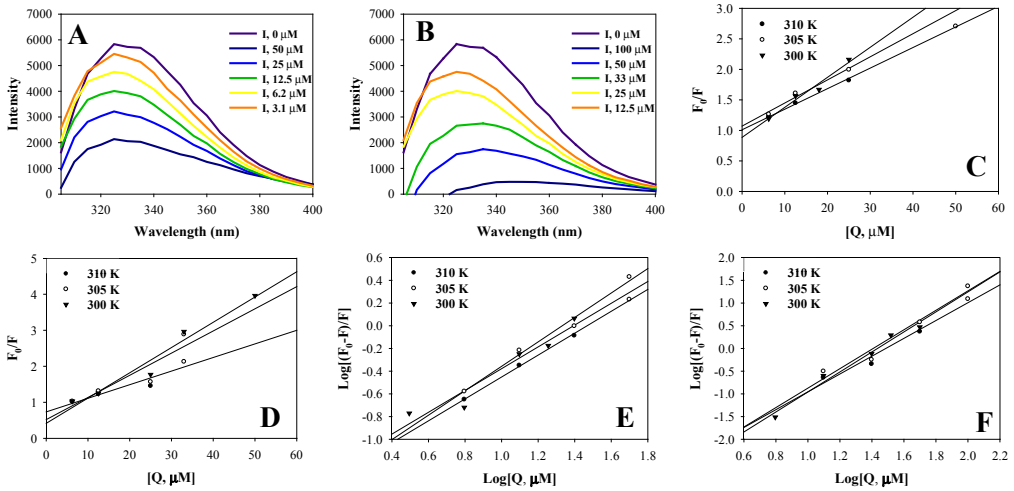

Fig. 3. The intrinsic fluorescence emission spectra of α-glucosidase (0.15 U/mL) in the absence or presence of compounds **4** (A) and **8** (B). The Stern–Volmer (C and D) and modified (E and F) plots of α-glucosidase fluorescence quenching at 300, 305, and 310 K, respectively.

18.5 ± 1.4 and 24.3 ± 2.1 μM (Fig. 2D and E and Table 1). These studies revealed that compounds **4** and **8** were anchored in an allosteric site of α-glucosidase, similar to cyanidin-3-*O*-β-glucoside (C3G) and cyanidin-3,5-*O*- β-diglucoside [17]. By comparison, anthocyanidin derivatives (**4** and **8**) had greater inhibitory activity than C3G.

2.2. Fluorescence quenching of α-glucosidase with anthocyanins

To obtain insight into binding of α-glucosidase with different concentrations of anthocyanins, enzyme-pigment mixtures were subjected to fluorescence spectroscopy scanning of emission wavelengths ranging from 305 to 400 nm, with an excitation wavelength of 280 nm at 300, 305, and 310 K.

As shown in Fig. 3A and B, the two fluorescence intensities of α-glucosidase had a remarkable decrease when mixed with anthocyanin derivatives **4** and **8** (at 300, 305, and 310 K). Sharp changes in the intrinsic fluorescence of α-glucosidase based on the concentration of the inhibitor could argue that these compounds are transformed directly into the tertiary structure of enzyme by impacting tryptophan or tyrosine residues. The emission spectra of enzymes by compound **4** maintained a maximum wavelength of 325 nm. However, three values from compound **8** were red shifted toward longer wavelengths. Therefore, compound **8** could lead to greater transformation of enzyme conformation than compound **4**.

Fluorescence quenching spectra values were converted by the linear regression with F_0/F vs. [Q] (Fig. 3C and D). Compound **4** showed *Ksv* values of 0.035, 0.0379, and 0.0451 Lμmol^{-1} at 310, 305, and 300 K, respectively. In addition, the *Ksv* values of compound **8** were 0.0377, 0.0615, and 0.0701 Lμmol^{-1} (Fig. 3C and D and Table 2). Furthermore, the plots of Log $[(F_0 - F)/F]$ vs. Log [Q] were used with the modified Stern–Volmer Eq. (3) to solve for the binding constant (K_b) and binding number (n) (Fig. 3E and F). In summary, K_b values of compound **4**, which had a 1:1 ratio of binding with α-glucosidase, were 0.0383 (310 K), 0.0368 (305 K), and 0.0458 (300 K) Lμmol^{-1}, respectively (Table 2). By contrast, K_b values for compound **8** when combined with a α-glucosidase were 0.0012, 0.0010, and 0.007 Lμmol^{-1} at 310, 305, and 300 K, respectively. These findings suggest that compound **4** had greater affinity for α-glucosidase compared with the interactive force of compound **8.**

Table 2
The quenching constants of α-glucosidase by anthocyanins **4** and **8**.

	Temperature (K)	*Ksv* (Lμmol^{-1})	K_b (Lμmol^{-1})	*n*
4	310	0.0350	0.0383	0.965
	305	0.0379	0.0368	1.076
	300	0.0451	0.0458	0.960
8	310	0.0377	0.0012	1.962
	305	0.0615	0.0010	2.142
	300	0.0701	0.0007	2.204

2.3. Molecular docking

To visualize the complex containing the receptor and ligand, we used *in silico* simulations of molecular docking. To find the allosteric site of the α-glucosidase bond with mixed noncompetitive inhibitors (**4** and **8**), we performed blind docking by setting up a grid containing all enzymes. The top 50 autodocking results out of 25 million iterations were extracted and clustered. Fig. 4A shows the predicted binding location. Compound **4** formed cluster with the most bonds at about −7.17 kcal/mol (Fig. 4B). In addition, compound **8** formed a cluster with the greatest number of bonds at the lowest energy of about −6.37 kcal/mol. We suggest that these locations are the allosteric site bonds for compounds **4** and **8** (Fig. 4C). Compound **4** often was composed of a main hydrogen bond with Gly155 (2.74 Å), Thr229 (3.07 Å), Lys231 (2.76 Å), Leu232 (3.33 Å), and Asn309 (2.63 Å), and π–π interaction with Phe306 (7.09 Å) (Fig. 4D and F and Table 3). The lowest autodock score of −6.37 kcal/mol for compound **8** was related to five hydrogen bonds with Gln61 (2.94 Å), Met64 (3.22 Å), Glu397 (2.72, 2.96 Å), and Trp469 (2.81 Å) (Fig. 4E and G and Table 3). The molecular docking was consistent with the above results of enzyme assays, kinetics, and fluorescence quenching studies. In particular, anthocyanidin **4** was close to Tyr308 and Tyr408, and anthocyanin **8** was located near Trp394, Tyr399, and Trp460. In this study, two compounds showed a correlation between molecular docking and bioactivity although they were bound at different positions in the receptor. Compound **4**, which bound at a lower energy than **8**, had a binding to a small cavity near the catalytic site. It may affect the flexible entrance for the substrate to pass through. Whereas, compound **8** bound to the allosteric site farther from the catalytic site than that of **4**. The above result suggested a sufficient explanation as to whether **4** was more potential inhibitor than **8**.

2.4. Molecular dynamics

α-Glucosidase with the potential inhibitor (**4**) or without was subjected to molecular dynamics in the 300 K and 1 bar to for 20 ns,

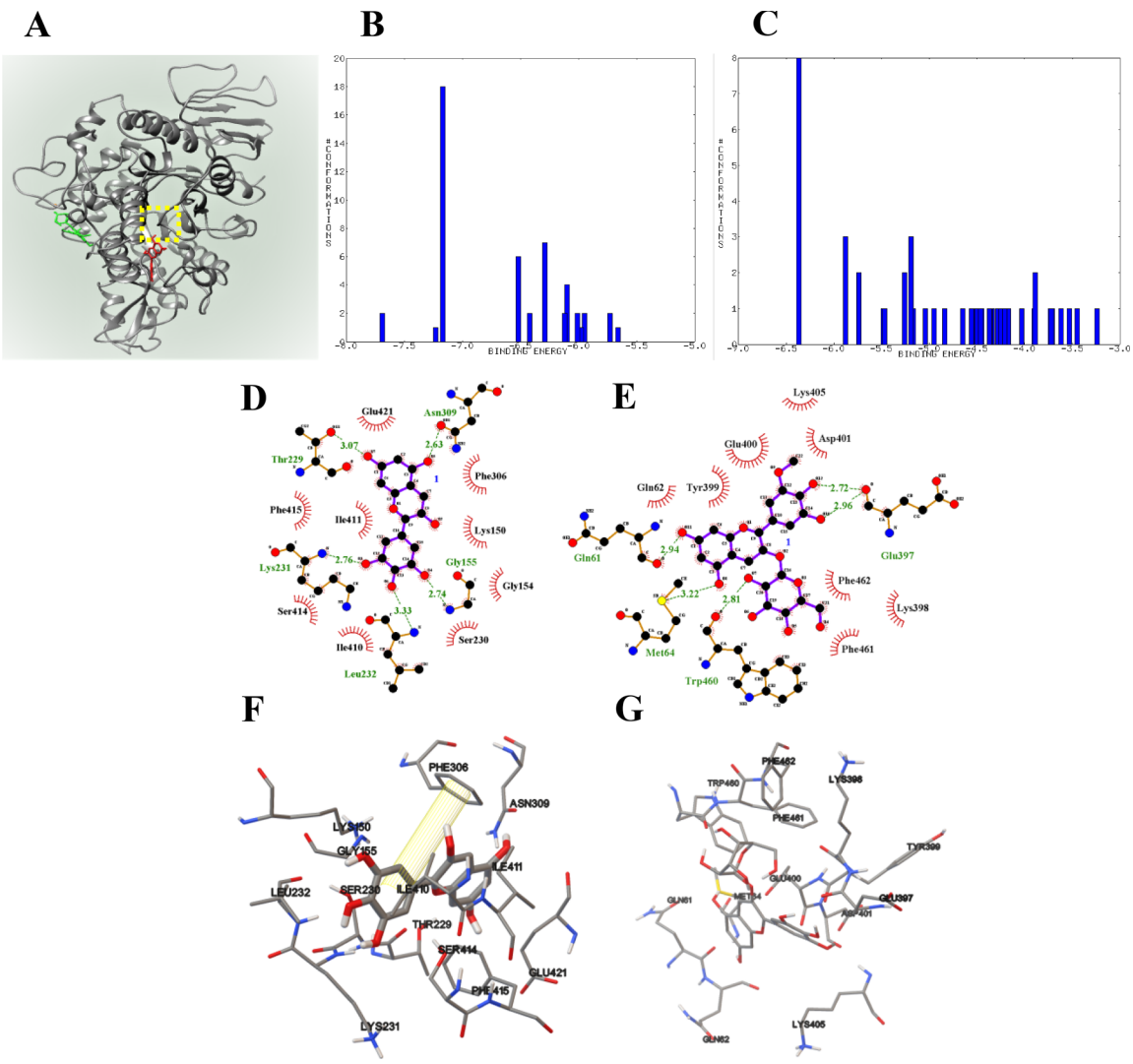

Fig. 4. (A) Best docking position of compounds **4** (red) and **8** (green) with α-glucosidase (yellow dot box: catalytic site). Clustering results of Autodock docking score of **4** (B) and **8** (C). The green dot and yellow tunnel line represent respective hydrogen bonds (D and E) and π–π interaction (F and G) between inhibitors (**4** and **8**) and residue in enzyme. (For interpretation of the references to colour in this figure legend, the reader is referred to the web version of this article.)

respectively. In Fig. 5A and B, the simulation results were visually represented by overlapping frames per 2-ns. Free α-glucosidase had a lower potential energy value than that of the ligand-enzyme complex (Fig. 5C). The root-mean-square-deviation (RMSD) of protein of them didn't show much difference under ~0.32 nm (Fig. 5D). Also, amino acid residues of these had the root-mean-square fluctuation (RMSF) of within ~0.5 nm. However, these of 261–265, 323–334, and 409–419 residues had significant differences (Fig. 5E). When inhibitor **4** had being combined into small capacity of receptor, they mainly composed of 0–3 hydrogen bonds (Fig. 5F). This affected the fluid shape change in the secondary structure of α-glucosidase with ligand compared to free enzyme (Fig. 6A and B). Also, the three groups, Asp228-Asn247, Glu277-Glu284, and Asp307-Val319, located for the entrance of catalytic site had different secondary structure. Among them, Asp228-Asn247 loop had a turn secondary structure rather than a bend of the original. Glu277-Glu284 that linked a α-helix to a β-sheet initially formed a turn and then a helix structure. On the other hand, the shape change of Asp307-Val319 group was insignificant (Fig. 6). As mentioned above, it was confirmed to show the difference of secondary structure between receptor and ligand-receptor for molecular dynamics. These results suggested that the degradation of the receptor by inhibitor (**4**) may possibly lower the binding force with the substrate.

3. Conclusion

This study evaluated the inhibitory activity of anthocyanin derivatives **1–8** on α-glucosidase. Delphinidin (**4**) and petunidin-3-*O*- β-glucoside (**8**) showed the greatest potential inhibitory activity, with IC_{50}

Table 3
Hydrogen bond analysis of inhibitor with α-glucosidase.

	Hydrogen bonds (Å)	Autodock Score (kcal/mol)
4	Gly155 (2.74), Thr229 (3.07), Lys231 (2.76), Leu232 (3.33), Asn309 (2.63),	−7.17
8	Gln61 (2.94), Met64 (3.22), Glu397 (2.72,2.96), Trp460 (2.81)	−6.37

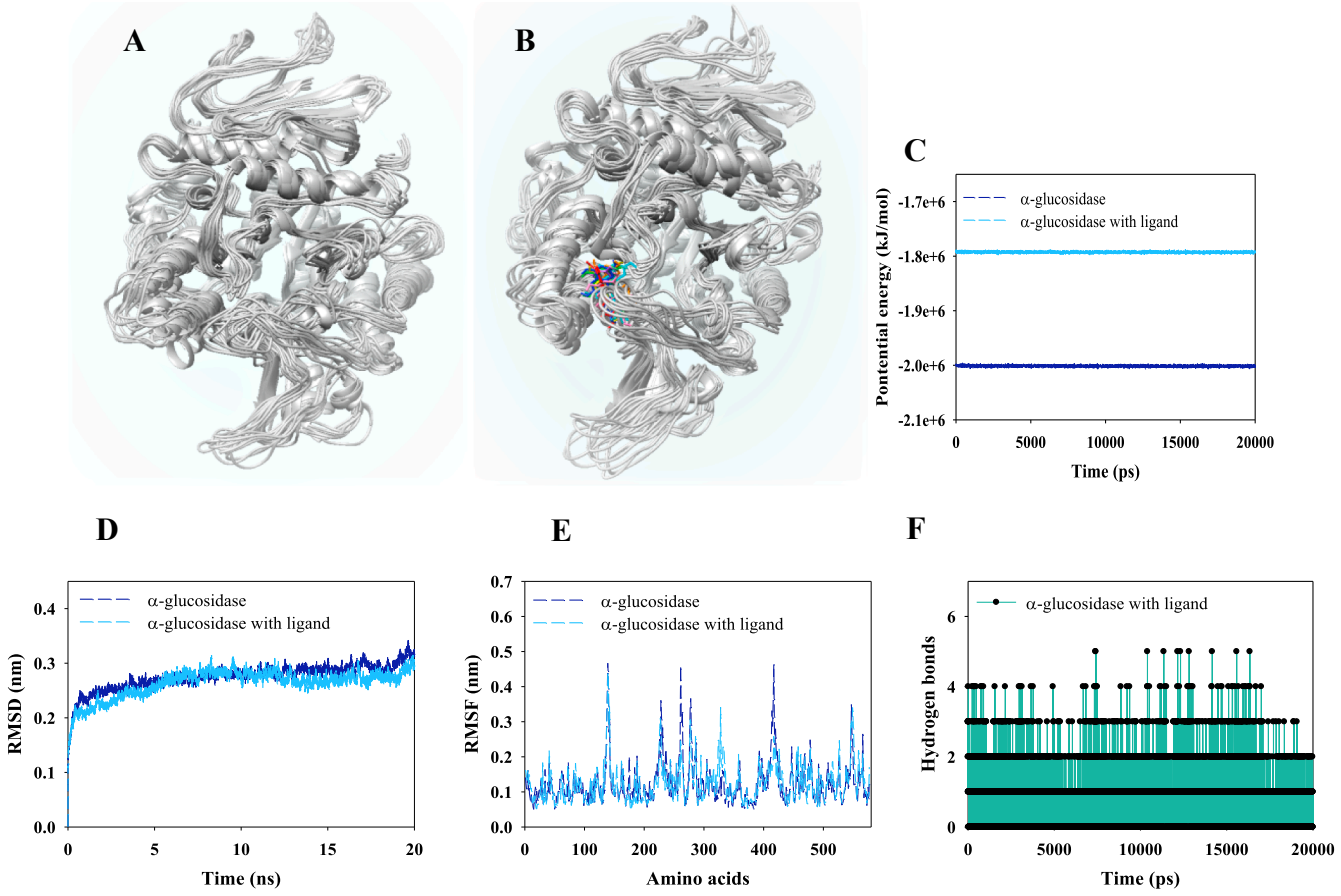

Fig. 5. Superpositions of α-glucosidase with compound **4** (**A**) and without (**B**) for simulation trajectory. The potential energy (**C**), RMSD (**D**), RMSF (**E**), hydrogen bonds (**F**) of simulation calculated for 20 ns.

values of 14.4 ± 0.1 and 29.7 ± 1.2 μM, respectively. Furthermore, these compounds are mixed with noncompetitive inhibitors that bind more with greater affinity to allosteric sites, with k_i values of 18.5 ± 1.4 and 24.3 ± 2.1 μM, respectively. Fluorescence quenching of α-glucosidase by anthocyanins was supported by the binding information of *Ksv*, K_b, and *n* values between their complexes. Molecular docking simulations allowed us to find predicted binding positions on the receptor. Inhibitors **4** and **8** have been suggested to have hydrogen bonds within 3.5 Å distance of Gly155, Thr227, Lys231, Leu232 and Asn309, (compound **4**) and Gln61, Met64, Glu397 and Trp460 (compound **8**). The potential inhibitor (**4**) influenced the structure of α-glucosidase, while the complex of ligand with receptor was calculated as GROMOS force field by molecular simulation. Therefore, delphinidin (**4**) and petunidin-3-*O*-β-glucoside (**8**) may be excellent potential inhibitors of α-glucosidase as targets for treating diabetes.

4. Materials and methods

4.1. General experimental procedures

Anthocyanin derivative **1** and **3–8** (**1**: 65999; **3**: 79457; **4**: 43725; **5**: 52976; **6**: 42739; **7**: 73705; **8**: 30638), α-glucosidase (G5003), acarbose (A8980), and 4-nitrophenyl-$_D$-glucopyranoside (N1377) were purchased from Sigma-Aldrich (St. Louis, MO, USA). Anthocyanidin **2** was purchased from LGC Standards (1154-78-5, Teddington Middlesex. UK). UV–Vis spectra were measured using a TECAN infinite 200 PRO® spectrophotometer (Zurich, Switzerland).

4.2. α-Glucosidase assay

To find potential α-glucosidase inhibitors, the eight anthocyanin derivatives were tested at 100 μM *in vitro* using enzyme assays, as described previously with some modification [18]. Briefly, we used 20 μL absence or presence of inhibitor in MeOH was mixed in 130 μL enzyme solution (0.1 mM phosphate buffer, pH 6.8), and then 50 μL 4-nitrophenyl-$_D$-glucopyranoside (1 mM) was added to the mixture. The converted product was monitored at UV–Vis 405 nm for 20 min.

The inhibitory activity rate was calculated according to the following equation:

$$\text{Inhibition rate } (\%) = [(\Delta C - \Delta I)/\Delta C] \times 100 \quad (1)$$

where ΔC and ΔI are the intensity of control and inhibitor, respectively, after 20 min.

4.3. Fluorescence quenching

Fluorescence spectra of α-glucosidase in the absence and presence of anthocyanins in MeOH were scanned with a TECAN infinite 200PRO® spectrophotometer at 300, 305, and 310 K. The blank was used for buffer spectrum values. The mixture of receptors with ligands was set at an excitation wavelength of 280 nm and an emission wavelength from 305 to 400 nm after incubation for 10 min. Fluorescence quenching of α-glucosidase by anthocyanin derivative was described by the Stern–Volmer equation:

$$F_0/F = 1 + K_{SV}[Q] \quad (2)$$

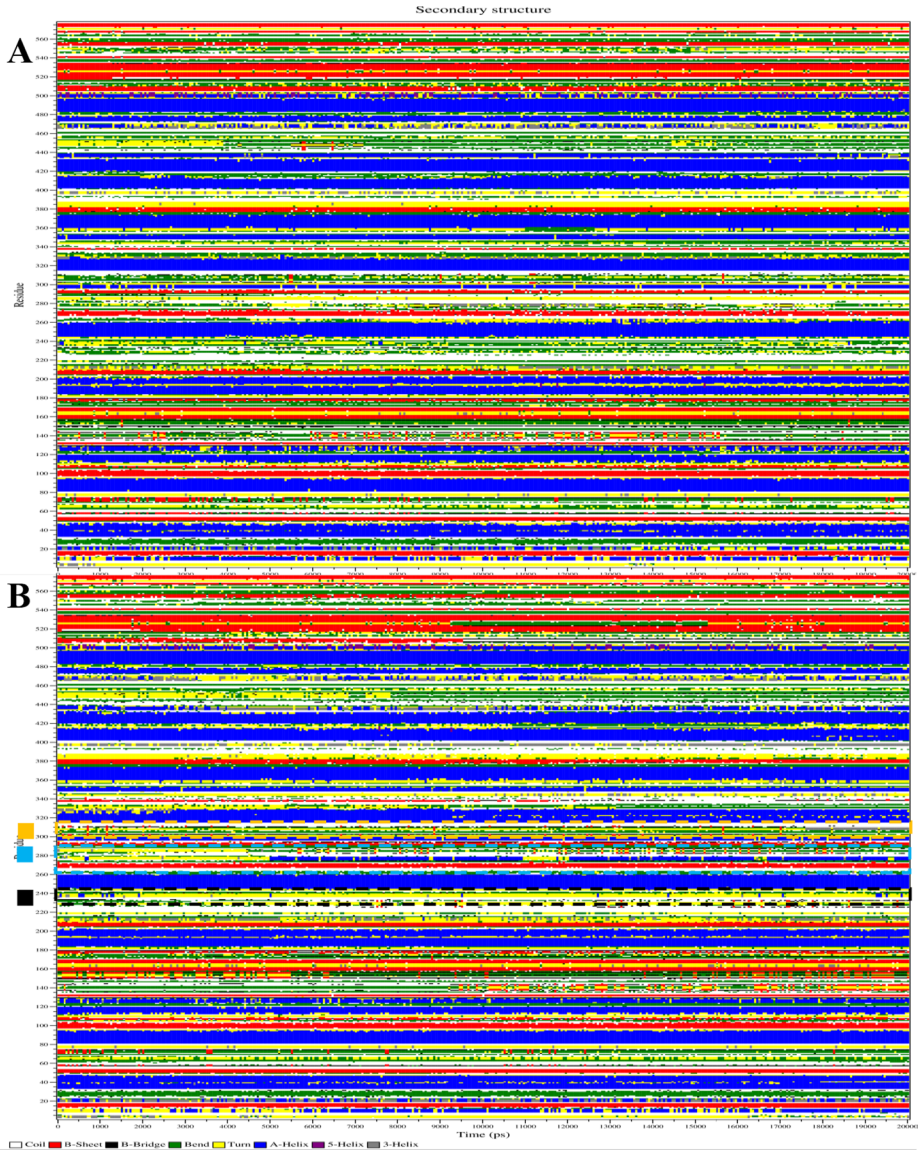

Fig. 6. Secondary structure changes in α-glucosidase with inhibitor **4** (A) or without (B) (black square: Asp228-Asn247; blue square: Glu277-Glu284; orange square: Asp307-Val319). (For interpretation of the references to colour in this figure legend, the reader is referred to the web version of this article.)

where F_0 and F represent the fluorescence values in the absence and presence of anthocyanins, respectively, [Q] is the concentration of ligands, and K_{SV} is the Stern–Volmer quenching constant.

The binding constant (K_b) and binding affinity (n) are calculated using a modified Stern–Volmer equation:

$$\mathrm{Log}[(F_0 - F)/F] = \mathrm{Log}K_b + n\mathrm{log}\ [Q] \quad (3)$$

4.4. Molecular docking

The 3D structure of α-glucosidase was constructed from homology modeling based on the scaffold of *Saccharomyces cerevisiae* isomaltase (pdb id: 3AJ7; NCBI, Rockville, MD, USA). The new enzyme structure was minimized by GROMOS96 force field in Gromacs package (ver. 4.6.5; Stockholm University, Stockholm, Sweden) [19]. For molecular docking, this enzyme, which had added with hydrogen atoms and assigned with Gasteiger charges, was contained in the grid with number points (xyz 150 × 180 × 150 at spacing 0.375) by using Autodocktools (ver. 4.2; The Scripps Research Institute, La Jolla, CA, USA). The ligand was detected at the torsion root and rotation bonds for flexible ligand docking. For searching the detailed binding position, molecular docking was iterated 25,000,000 times with the Lamarckian genetic algorithm [20]. These results were converted to a score and figure using Autodocktools and Chimera (University of California, San Francisco, CA, USA) and LigPlot (Cambridge, UK) software programs.

4.5. Molecular dynamics

Molecular dynamics were performed to simulate the complex of α-glucosidase with inhibitor **4** or without by the Gromacs 4.6.5 software. Files of inhibitor (**4**) relating with molecular simulation were produced to The GlycoBioChem PRODRG2 Server. Also, these of α-glucosidase were generated by g_utility in Gromacs 4.6.5 package. The sources of ligand files were added in files of enzyme. Revised gro. file was solvated in water molecules of a cubic box with a size of 11 × 11 × 11 containing six sodium ions (1.0 Å distance). And then this complex was minimized until the maximal force of 10 kJ/mol. NVT and NPT were simulated at 300 K temperature and 1 bar pressure for 100 ps in the order, respectively. Finally, the complex was performed to MD simulation for 20,000 ps.

4.6. Statistical analysis

Data are expressed as the means ± standard deviation (n = 3). All values were analyzed using Sigma plot to determine variation among treatments.

Acknowledgements

This research was supported by Radiation Technology R&D program (No. 2017M2A2A6A05018541) through the National Research Foundation of Korea (NRF) funded by the Ministry of Science, ICT & future Planning.

Conflicts of Interest

The authors declare no conflict of interest.

Appendix A. Supplementary material

Supplementary data to this article can be found online at https://doi.org/10.1016/j.bioorg.2019.01.033.

References

[1] B. Šmídová, D. Šatínský, K. Dostálová, P. Solich, Talanta 166 (2017) 249–254.
[2] F. Zhu, Food Res. Int. 109 (2018) 232–249.
[3] C. Carrillo, C. Buvé, A. Panozzo, T. Grauwet, M. Hendrickx, Food Chem. 227 (2017) 271–279.
[4] C. Grajeda-lglesias, E. Salas, N. Barouh, B. Baréa, M.C. Figueroa-Espinoza, Food Chem. 230 (2017) 189–194.
[5] J. Sun, M. Li, F. Zou, S. Bai, X. Jiang, L. Tian, S. Ou, R. Jiao, W. Bai, Food Chem. Toxicol. 119 (2018) 268–274.
[6] T. Suantawee, H. Cheng, S. Adisakwattana, Inter. J. Biol. Macromol. 93 (2016) 814–821.
[7] A. Castañeda-Ovando, M.D.L. Pacheco-Hernández, M.E. Páez-Hernández, J.A. Rodríguez, C.A. Galán-Vidal, Food Chem. 113 (2009) 859–871.
[8] Y. Sivasothy, L.K. Yong, L.K. Hoong, M. Litaudon, K. Awang, Phytochemistry 122 (2016) 265–269.
[9] S. Imran, M. Taha, N.H. Ismail, S.M. Kashif, F. Rahim, W. Jamil, M. Hariono, M. Yusuf, H. Wahab, Eur. J. Med. Chem. 105 (2015) 156–170.
[10] World Health Organization, Dementia. http://www.who.int/mediacentre/factsheets /fs362/en/, 2017 (accessed 20 September 2018).
[11] E. Richard, M.D. Pratley, Am. J. Med. 126 (2013) S2–S9.
[12] D. Şöhretoğlu, S. Sari, B. Barut, A. Özel, Bioorg. Chem. 79 (2018) 257–269.
[13] C. Proença, M. Freitas, D. Ribeiro, E.F.T. Oliveira, J.L.C. Sousa, S.M. Tomé, M.J. Ramos, A.M.S. Silva, P.A. Fernandes, E. Fernandes, J. Enzyme Inhib. Med. Chem. 32 (2017) 1216–1228.
[14] H.E. Khoo, A. Azlan, S.T. Tang, S.M. Lim, Food Nutr. Res. 61 (2017) 1361779.
[15] D. Kalita, D.G. Holm, D.V. LaBarbera, J.M. Petrash, S.S. Jayanty, PLoS One 13 (2018) e0191025.
[16] Q. You, F. Chen, X. Wang, P.G. Luo, Y. Jiang, J. Agric. Food Chem. 59 (2011) 9506–9511.
[17] H. He, Y.-H. Lu, J. Agri. Food Chem. 61 (2013) 8110–8119.
[18] L. Zhang, Z.-C. Tu, T. Yuan, H. Wang, X. Xie, Z.-F. Fu, Food Chem. 208 (2016) 61–67.
[19] J.H. Kim, C.W. Cho, H.Y. Kim, K.T. Kim, G.-S. Choi, H.-H. Kim, I.S. Cho, S.J. Kwon, S.-K. Cho, J.-Y. Yoon, S.Y. Yang, J.S. Kang, Y.H. Kim, Inter. J. Biol. Macromol. 102 (2017) 960–969.
[20] M. Taha, S.A.A. Shah, M. Afifi, S. Imran, S. Sultan, F. Rahim, K.M. Khan, Bioorg. Chem. 77 (2018) 586–592.